Effect of zoledronic acid therapy in an *in vivo* model of bone invasive feline oral squamous cell carcinoma

[1]Chelsea K Martin

Abstract

Objective: To test the hypothesis that zoledronic acid will inhibit tumor-induced osteolysis and reduce tumor growth and invasion in a xenograft mouse model of bone invasive oral squamous cell carcinoma (OSCC). In humans, OSCC is the 6th most common cancer in the world. Bone invasion frequently occurs and is associated with poor prognosis and reduced survival. OSCC is the most commonly diagnosed malignancy of the oral cavity in cats and has a grave prognosis with an average duration of survival of only 2 months. Feline OSCC (FOSCC) is very aggressive and commonly invades bone, which is characterized by osteoclastic bone resorption. Zoledronic acid (ZOL) is a potent third generation nitrogen-containing bisphosphonate which inhibits osteoclastic bone resorption. There are currently no available treatment modalities which significantly improve prognosis or prolong survival of cats with FOSCC. Methods: A luciferase-expressing FOSCC cell line (SCCF2Luc) was injected into the perimaxillary subgingival lamina propria of 30 athymic nude mice. Mice were treated with 100 µg/kg ZOL, or vehicle, twice weekly for 4 weeks. Thirty non-tumor-bearing mice served as controls. Tumor growth was monitored with *in vivo* bioluminescent imaging and tumor dimensions were determined with calipers. The degree of bone loss was evaluated using faxitron radiography and micro-computed tomography (microCT). A 2mm thick region of interest (ROI) in the rostral skull, incorporating the xenograft and adjacent pre-maxillary and maxillary bone, was selected using µCT and image analysis software. ROI-bone surface area and bone volume were calculated and compared

[1] 349 Goss Laboratory, 1925 Coffey Rd, Columbus, OH, 43210. The author is grateful for the guidance of Thomas Rosol (research advisor), for the assistance of laboratory colleagues Jillian Werbeck, Nandu Thudi, Lisa Lanigan, Tobie Wolfe and Ramiro Toribio; and microCT technical support from Michelle Carlton (Department of Radiology).

between treatment groups. Tumor invasiveness was evaluated microscopically. Osteolysis and osteoclast activation were evaluated with TRAP histochemistry and histomorphometry. Results and conclusions: Progressive xenograft growth occurred in all mice, as indicated by increasing bioluminescence. Bioluminescence was positively correlated with tumor volume. ZOL treatment significantly reduced tumor growth (*in vivo* bioluminescence), prevented loss of bone volume and surface area (microCT), and was associated with reduced osteolysis and increased periosteal new bone formation (microCT, faxitron radiography and histomorphometry). ZOL had no effect on tumor invasion around the incisor or into the nasal cavity. ZOL-mediated inhibition of tumor-induced osteolysis was characterized by significantly reduced numbers of TRAP-positive osteoclasts at the tumor-bone interface and was associated with osteoclast vacuolar degeneration. The ratio of eroded to total bone surface was not significantly affected by treatment; indicating that ZOL-mediated inhibition of osteolysis was independent of osteoclast activation and maturation.

Significance: This preclinical model of OSCC recapitulates the bone invasive phenotype characteristic of the disease in both humans and cats, and will be useful to future preclinical studies of bone invasive OSCC regardless of species. ZOL reduced FOSCC-induced osteolysis and bioluminescence, but invasive behavior was unchanged. The results of this experiment suggest that ZOL monotherapy would be of limited clinical use in the management of FOSCC, but may be valuable as adjunct therapy with the purpose of maintaining mandibular and maxillary bone volume and function.

Introduction

Squamous cell carcinoma is the most common form of oral cancer in both humans (1-3) and domestic cats (4-5). Destruction and invasion of mandibular and maxillary bone frequently

occurs and contributes to morbidity and mortalilty (6, 7). Feline oral squamous cell carcinoma (FOSCC) is the most commonly diagnosed tumor of the oral cavity in cats. It is an extremely aggressive cancer characterized by profound destruction of oral tissues and frequently invades bone (8). Surgical removal may be curative in early cases but is associated with significant morbidity (9, 10), or their tumors are so extensive that they are no longer surgical candidates (8). FOSCC-associated bone destruction contributes significantly to patient morbidity and mortality.

The mechanism of FOSCC-induced osteoclastic bone resorption is unknown. We hypothesize that FOSCC invasion into bone is facilitated by a vicious cycle of tumor growth and bone resorption which can be abrogated by targeting bone-resorbing osteoclasts. The vicious cycle theory was originally described in human breast cancer bone metastasis as a relationship between the tumor-derived PTHrP (agonist of osteoclastic bone resorption) and bone derived TGF-β (stimulates tumor-expression of PTHrP with increased tumor growth and invasion) (11), however other OSCC-derived cytokines may contribute to osteolysis, including prostaglandin E2 (PGE2) (12, 13), parathyroid hormone related-protein (PTHrP), tumor necrosis factor-alpha (TNF-α), interleukin-6 and interleukin-11 (14-16).

Regardless of the number and type of bone resorption agonists expressed by FOSCC cells, tumor-associated osteoclastic bone resorption can be inhibited by nitrogen-containing bisphosphonates (NBPs). NBPs such as zoledronic acid (ZOL) inhibit osteoclasts by inhibiting farnesyl pyrophosphate synthase in the mevalonate (MVA) pathway (17, 18). Inhibition of the MVA pathway leads to reduced prenylation of small guanosine-triphosphate (GTP)-binding proteins (Rab, Rac and Rho) responsible for osteoclast function and results in osteoclast apoptosis (19, 20). We hypothesize that inhibition of osteoclastic bone resorption with ZOL will not only reduce bone loss but will also inhibit OSCC xenograft growth and invasion by

antagonizing the vicious cycle of osteolysis and tumor progression.

We have designed a novel bone-invasive, bioluminescent orthotopic xenograft nude mouse model of FOSCC using cells derived from a bone invasive FOSCC. The inhibitory activity of ZOL on FOSCC growth and associated osteolysis was investigated using bioluminescent imaging, radiographs, micro-computed tomography and maxillary histomorphometry. We found that ZOL may be an effective treatment for preventing bone resorption in FOSCC.

Materials and Methods

Cells and reagents. SCCF2 cells were derived from a bone-invasive gingival squamous cell carcinoma of a 7-year old male castrated domestic shorthaired cat using methods previously described (21). Zoledronic acid (Zometa; Novartis) was purchased from the James Cancer Center at The Ohio State University. ZOL vehicle was prepared according to the package insert and consisted of 44 mg/ml mannitol and 4.8 mg/ml sodium acetate in sterile water.

Transfection of SCCF2 cells with luciferase gene. SCCF2 cells were stably transfected with a plasmid containing a luciferase-yellow fluorescent protein (YFP) fusion construct (pCDNA3.1(+).yLuc-YFP) using Lipofectamine™ LTX and PLUS™ Reagent (Invitrogen) according to the manufacturer's instructions. Luciferase expression of individual colonies was determined using the Xenogen IVIS 200 system in growth medium supplemented with 142.5 μg/ml D-Luciferin (Xenogen, Alameda, CA). Three colonies with the highest bioluminescence were pooled to create the luciferase-expressing cell line SCCF2Luc.

Animals and treatments. Animal procedures were approved by the Institutional Lab Animal Care and Use Committee. Sixty 6-week-old male nu/nu mice (NCI, Frederick, MD) were randomly assigned to 1 of 4 groups; non tumor-bearing vehicle-treated mice, tumor-bearing vehicle-treated mice, non tumor-bearing ZOL-treated mice and tumor-bearing ZOL-treated mice. Mice were

anesthetized with isofluorane and injected with $1x10^6$ SCCF2Luc cells in 0.1ml PBS, subgingivally, adjacent to the maxilla. Non-tumor bearing mice were injected with cell-free PBS. Treatment was initiated 7 days following SCCF2Luc injection, and consisted of twice weekly subcutaneous injections of 100 μg/kg ZOL or vehicle. Bioluminescent images were collected 1,7,21 and 28 days following the initiation of treatment. Mice were sacrificed on day 28 and blood was collected for determination of PTHrP and total calcium levels.

Bioluminescent imaging. Bioluminescent imaging was done with the *in vivo* imaging system (IVIS, Caliper Life Sciences) as previously described (22). Photon signals were quantified with LivingImage software version 2.2 (Caliper life sciences).

Faxitron radiography and micro-computed tomography. The mandible was removed from each skull and the degree of maxillary and premaxillary bone loss was evaluated qualitatively using a Faxitron cabinet X-ray system (Hewlett-Packard, McMinnville, OR). Bone loss was evaluated quantitatively using micro-computed tomography (microCT, Inveon, Siemens AG, Munich, Germany). Image data was reconstructed using Cobra software (Exxim, Pleasanton CA) and analyzed using Inveon 3D analysis software. Intensity thresholds were determined for selecting bone from surrounding soft tissue and were kept constant for all mice. Bone surface area and bone volume were determined for a 2 mm thick ROI in the region of xenograft growth and compared between treatment groups.

Histopathology, TRAP histochemistry and histomorphometry. Skulls were routinely fixed and decalcified. Enzymatic histochemistry for tartrate-resistant acid phosphatase (TRAP, Sigma-Aldrich) was done as previously described (23). Bone histomorphometry was done with Imagescope software (Aperio). Percentage of eroded bone, percentage of bone in contact with activated osteoclasts, number of activated osteoclasts, and average osteoclast length were

determined for treated and untreated tumor-bearing mice. Only sections with a minimum of 3mm of direct tumor-bone interface were included. Tissues were also evaluated for the presence of tumor invasion around the maxillary incisor and into the nasal cavity.

Plasma PTHrP and Calcium. Plasma PTHrP (1-86) was measured using a commercially available two-site immunoradiometric assay (Diagnostic Systems Laboratories Inc., Webster, TX, USA). Plasma calcium concentration was determined using a commercially available calcium assay kit (Bioassay Systems, Hayward, CA). Both assays were performed according to the manufacturer's instructions.

Statistical analysis. Results are displayed as means with standard deviation. Normally distributed data were analyzed using Student's t-test or one-way ANOVA with Bonferroni's post hoc test. Data not normally distributed was evaluated with Wilcoxon rank sum (Mann-Whitney) test. P values less than 0.05 were considered statistically significant. Categorical data was analyzed using Fishers exact test. All analysis were performed with STATA intercooled 10 (Cary, NC).

Results

ZOL treatment reduced tumor growth but not rate of invasion. Progressive xenograft growth was observed in all mice. Radiance values were normalized by dividing measurements on days 7, 21 and 28 by radiance of day 1 and expressed as fold change radiance. At the 28th day, ZOL treatment reduced fold change radiance by 43% compared to the vehicle-treated mice (P=0.004, figure 1). Histomorphometry revealed that ZOL-treatment reduced adjusted tumor area (total area minus areas of necrosis) by 14% (P=0.0375, figure 2). Bioluminescent imaging was more sensitive than calculating tumor volume from caliper measurements (data not shown) or histomorphometric evaluation of tumor area. Tumor invasion around the maxillary incisor was observed in 13 of 15 vehicle treated mice, and invasion into the nasal cavity was observed in 12

of 15 mice. The incidence of invasion did not significantly differ in ZOL treated mice.

Zoledronic acid reduces bone resorption. ZOL qualitatively reduced radiographic evidence of osteolysis and increased periosteal new bone formation in the region of xenograft growth (figure 3). MicroCT revealed that xenograft growth in vehicle treated mice was associated with a 13.9% loss of bone surface area ($P<0.0001$) and an 18.9% reduction in bone volume ($P<0.0001$, figure 4). ZOL-treatment prevented statistically significant loss of bone surface area and bone volume.

Histologic examination revealed that ZOL-treated mice retained more bone than vehicle-treated mice (figure 5). Maxillary histomorphometry demonstrated that SCCF2Luc xenograft growth was associated with a 47.7% reduction in total bone area (preexisting bone and new bone combined) compared to the non-tumor bearing side ($P=0.0002$), whereas ZOL treatment prevented loss of total bone area (figure 6). Loss of preexisting bone was reduced from 64.1% in untreated mice to 33.3% in ZOL-treated mice ($P=0.005$, figure 6). The preservation of total bone in ZOL-treated mice, as detected by microcomputed tomography and histomorphometry, is attributed to reduced loss of preexisting bone and increased new bone formation.

Zoledronic acid treatment resulted in fewer osteoclast numbers with vacuolar degeneration. Histomorphometric evaluation of TRAP-stained slides revealed no difference in the ratio of eroded to total bone surface between ZOL and vehicle treated mice, suggesting that xenograft-mediated recruitment and maturation of osteoclasts and initiation of bone resorption was not affected by ZOL-treatment. ZOL reduced the percentage of bone surface in direct contact with osteoclasts by 33.4% ($P=0.017$, figure 7). ZOL reduced the number of osteoclasts per millimeter by 51.8% ($P=0.0001$). The average osteoclast length was increased in the ZOL-treated mice by 39.1% ($P=0.0001$), which was characterized by cytoplasmic dilation with numerous, variably sized, circular, clear cytoplasmic vacuoles (vacuolar degeneration, figure 8).

ZOL failed to reduce plasma PTHrP in tumor bearing mice. Xenograft growth and ZOL-treatment had no effect on plasma calcium compared to control mice. Plasma PTHrP was elevated in tumor bearing mice (2.42 pM) compared to control mice (0.65pM, P=0.037, figure 9); however ZOL treatment did not significantly reduce plasma PTHrP values.

Discussion

Prior to this study, there have been no preclinical models which recapitulate the bone invasive behavior of FOSCC in which to evaluate therapeutic agents. We have designed a novel, bone invasive, bioluminescent orthotopic xenograft nude mouse model of OSCC using feline cells derived from a bone invasive FOSCC, and have demonstrated that ZOL treatment effectively reduced tumor growth and bone resorption associated with FOSCC xenograft growth.

SCCF2Luc xenografts induced osteoclastic bone resorption characterized by numerous activated osteoclasts at the tumor-bone interface. The mechanism by which FOSCC stimulates osteoclastic bone resorption is unknown, however we hypothesize that FOSCC invasion into bone is facilitated by a vicious cycle of tumor growth and bone resorption. Chirgwin and Guise (11) first proposed that osteolytic breast cancer metastasis in humans results from a relationship between tumor-derived PTHrP and bone derived TGF-β. Virtually all squamous cell carcinomas produce PTHrP (24, 25), including those of the feline oral cavity (21). We have used immunohistochemistry to demonstrate that spontaneous FOSCC tumors express PTHrP, and that the degree of PTHrP positivity increases in tumors associated with bone resorption (unpublished data). TGF-β causes increased secretion of PTHrP from tumor cells, and is known to increase FOSCC-expression of PTHrP *in vitro* (21). It is widely recognized that PGE_2 stimulates osteoclastogenesis through the up-regulation of RANKL expression in osteoblasts and bone marrow stromal cells (26). In human OSCC, high levels of PGE2 are due to up-regulation of

COX-2 (27), which is also over-expressed in OSCC of cats (28, 29).

ZOL therapy may have reduced xenograft growth indirectly by inhibiting the vicious cycle through inhibition of osteoclastic bone resorption, or through direct antineoplastic mechanisms. Preclinical research suggests that bisphosphonates may exert antitumor effects by inhibiting cancer cell adhesion, invasion, viability and angiogenesis (30-32). The inhibitory effect of bisphosphonates on angiogenesis may be the result of reduced circulating levels of VEGF. ZOL acid therapy has been shown to reduce circulating VEGF in humans with metastatic bone disease (33), and in a preliminary clinical trial in cats with OSCC (34). Early clinical reports have demonstrated that human cancer patients benefit from reduced skeletal metastasis and improved prognosis when bisphosphonates are included in their treatment regimens (33). A third generation bisphosphonate (YM529) prevented bone invasion and inhibited tumor growth in a syngeneic mouse model of OSCC (16).

ZOL inhibits osteoclastic bone resorption by inducing osteoclastic apoptosis through impaired prenylation of small GTPases as a result of farnesyl transferase inhibition (17, 18). Our study revealed that osteoclasts in ZOL treated mice continued to form and maintained their ability to resorb bone, but existed in reduced numbers and demonstrated evidence of vacuolar degeneration. The mechanism of this vacuolar degeneration is not known, however a study by Coxon et al. (2003) demonstrated that targeted inhibition of the small GTPase Rab resulted in altered osteoclast morphology characterized by dome shaped cells with large intracellular vacuoles (35). They reported that the antiresorptive properties of the Rab inhibitor were likely due to disruption of Rab-dependent intracellular membrane trafficking in osteoclasts.

ZOL significantly reduced bone resorption in this model of bone-invasive OSCC; however ZOL failed to completely inhibit osteoclastic bone resorption. Tumor bearing mice continued to

lose preexisting bone in the face of ZOL therapy, albeit at a reduced level. A recent *in vitro* study revealed that a human OSCC cell line was capable of reducing osteoclast apoptosis through down regulation of the pro-apoptotic factor BIM (36). Osteoclasts in the SCCF2Luc tumor-bone microenvironment may have been partially protected from the proapoptotic effects of ZOL by factors produced by FOSCC cells.

Hypercalcemia associated with elevated circulating PTHrP has been occasionally reported in people with oral squamous cell carcinoma; but is rarely observed in cats with FOSCC. Plasma PTHrP levels were mildly elevated in mice bearing SCCF2Luc xenografts (attributed to xenograft production of PTHrP), but there was no associated increase in total calcium. Although there was no evidence of a humoral role of PTHrP in this model, PTHrP may have functioned in a paracrine manner to stimulate osteoclastic bone resorption.

Various adverse effects have been reported for NBP therapy; although osteonecrosis of the jaw (ONJ) has warranted the most concern. ONJ is characterized by exposed, necrotic jaw bone and has been observed in patients treated with NBPs (37). The incidence of ONJ among human patients receiving intravenous NBP therapy is 5 - 10% (38). In this study, ZOL was well tolerated in both the tumor-bearing and non-tumor bearing mice and there was no evidence of ONJ, however longer studies are required to fully characterize the risk of developing ONJ.

This preclinical model of OSCC recapitulates the bone invasive phenotype characteristic of the disease in both humans and cats, and will be useful to future preclinical studies of bone invasive OSCC regardless of species. ZOL reduced FOSCC-induced osteolysis and bioluminescence, but invasive behavior was unchanged. The results of this experiment suggest that ZOL monotherapy would be of limited efficacy in the management of FOSCC, but may be valuable as adjunct therapy with the purpose of maintaining mandibular and maxillary bone volume and function.

References

1. Neville B,W., Damm D,D., Allen C,M., Bouquot J,E., editors. Oral & maxillofacial pathology. 2nd ed. Philadelphia, Pennsylvania: Saunders; 2002.

2. Silverman S, Jr., editor. Oral cancer. 4th ed. Hamilton, Ontario, Canada: BC Decker Inc.; 1998.

3. Silverman S,Jr. Demographics and occurrence of oral and pharyngeal cancers. the outcomes, the trends, the challenge. J Am Dent Assoc 2001;132 Suppl:7S-11S.

4. Dorn CR, Priester WA. Epidemiologic analysis of oral and pharyngeal cancer in dogs, cats, horses, and cattle. J Am Vet Med Assoc 1976;169(11):1202-6.

5. Stebbins K, E., Morse C, C., Goldschmidt MH. Feline oral neoplasia: A ten-year survey. Vet Pathol 1989;26(2):121-8.

6. Patel RS, Dirven R, Clark JR, Swinson BD, Gao K, O'Brien CJ. The prognostic impact of extent of bone invasion and extent of bone resection in oral carcinoma. Laryngoscope 2008;118(5):780-5.

7. Shaw RJ, Brown JS, Woolgar JA, Lowe D, Rogers SN, Vaughan ED. The influence of the pattern of mandibular invasion on recurrence and survival in oral squamous cell carcinoma. Head Neck 2004;26(10):861-9.

8. Morris J, Dobson J. Head and neck. In: Morris J, Dobson J, editors. Small Animal Oncology. Alder Press Ltd, Oxford: Blackwell Science Ltd.; 2001. p. 94-124.

9. Hutson C, A., Willauer C, C., Walder E, J., Stone J, L., Klein MK. Treatment of mandibular squamous cell carcinoma in cats by use of mandibulectomy and radiotherapy: Seven cases (1987-1989). J Am Vet Med Assoc 1992;201(5):777-81.

10. Northrup NC, Selting KA, Rassnick KM, et al. Outcomes of cats with oral tumors treated with mandibulectomy: 42 cases. J Am Anim Hosp Assoc 2006;42(5):350-60.

11. Chirgwin J, M., Guise TA. Molecular mechanisms of tumor-bone interactions in osteolytic metastases. Crit Rev Eukaryot Gene Expr 2000;10(2):159-78.

12. Karmali RA, Wustrow T, Thaler HT, Strong EW. Prostaglandins in carcinomas of the head and neck. Cancer Lett 1984;22(3):333-6.

13. Jung TT, Berlinger NT, Juhn SK. Prostaglandins in squamous cell carcinoma of the head and neck: A preliminary study. Laryngoscope 1985;95(3):307-12.

14. Shibahara T, Nomura T, Cui NH, Noma H. A study of osteoclast-related cytokines in mandibular invasion by squamous cell carcinoma. Int J Oral Maxillofac Surg 2005;34(7):789-93.

15. Okamoto M, Hiura K, Ohe G, et al. Mechanism for bone invasion of oral cancer cells mediated by interleukin-6 in vitro and in vivo. Cancer 2000;89(9):1966-75.

16. Cui N, Nomura T, Noma H, et al. Effect of YM529 on a model of mandibular invasion by oral squamous cell carcinoma in mice. Clin Cancer Res 2005;11(7):2713-9.

17. Dunford JE, Thompson K, Coxon FP, et al. Structure-activity relationships for inhibition of farnesyl diphosphate synthase in vitro and inhibition of bone resorption in vivo by nitrogen-containing bisphosphonates. J Pharmacol Exp Ther 2001;296(2):235-42.

18. Kavanagh KL, Guo K, Dunford JE, et al. The molecular mechanism of nitrogen-containing bisphosphonates as antiosteoporosis drugs. Proc Natl Acad Sci U S A 2006;103(20):7829-34.

19. Hall A. Rho GTPases and the actin cytoskeleton. Science 1998;279(5350):509-14.

20. Luckman SP, Hughes DE, Coxon FP, Graham R, Russell G, Rogers MJ. Nitrogen-containing bisphosphonates inhibit the mevalonate pathway and prevent post-translational prenylation of GTP-binding proteins, including ras. J Bone Miner Res 1998;13(4):581-9.

21. Tannehill-Gregg S, Kergosien E, Rosol TJ. Feline head and neck squamous cell carcinoma cell line: Characterization, production of parathyroid hormone-related protein, and regulation by transforming growth factor-beta. In vitro cellular & developmental biology.Animal 2001;37(10):676-83.

22. Tannehill-Gregg SH, Levine AL, Nadella MVP, Iguchi H, Rosol TJ. The effect of zoledronic acid and osteoprotegerin on growth of human lung cancer in the tibias of nude mice. Clin Exp Metastasis 2006;23(1):19-31.

23. Thudi NK, Martin CK, Nadella MV, et al. Zoledronic acid decreased osteolysis but not bone metastasis in a nude mouse model of canine prostate cancer with mixed bone lesions. Prostate 2008;68(10):1116-25.

24. Grone A, Werkmeister J, R., Steinmeyer C, L., Capen C, C., Rosol TJ. Parathyroid hormone-related protein in normal and neoplastic canine tissues: Immunohistochemical localization and biochemical extraction. Vet Pathol 1994;31(3):308-15.

25. Danks J, A., Ebeling P, R., Hayman J, et al. Parathyroid hormone-related protein: Immunohistochemical localization in cancers and in normal skin. Journal of bone and mineral research : the official journal of the American Society for Bone and Mineral Research 1989;4(2):273-8.

26. Ono K, Akatsu T, Murakami T, et al. Involvement of cyclo-oxygenase-2 in osteoclast formation and bone destruction in bone metastasis of mammary carcinoma cell lines. J Bone Miner Res 2002;17(5):774-81.

27. Chan G, Boyle JO, Yang EK, et al. Cyclooxygenase-2 expression is up-regulated in squamous cell carcinoma of the head and neck. Cancer Res 1999;59(5):991-4.

28. Hayes A, Scase T, Miller J, Murphy S, Sparkes A, Adams V. COX-2 expression in feline oral squamous cell carcinoma (FOSCC)-an immunohistochemical study and analysis of survival. Vet Comp Onc 2005;3(1):44--45.

29. Hayes A, Scase T, Miller J, Murphy S, Sparkes A, Adams V. COX-1 and COX-2 expression in feline oral squamous cell carcinoma. J Comp Pathol 2006;135(2-3):93-9.

30. Santini D, Schiavon G, Angeletti S, et al. Last generation of amino-bisphosphonates (N-BPs) and cancer angio-genesis: A new role for these drugs? Recent Patents Anticancer Drug Discov 2006;1(3):383-96.

31. Dass CR, Choong PF. Zoledronic acid inhibits osteosarcoma growth in an orthotopic model. Mol Cancer Ther 2007;6(12 Pt 1):3263-70.

32. Guise TA. Antitumor effects of bisphosphonates: Promising preclinical evidence. Cancer Treat Rev 2008;34 Suppl 1:S19-24.

33. Lipton A. Emerging role of bisphosphonates in the clinic--antitumor activity and prevention of metastasis to bone. Cancer Treat Rev 2008;34 Suppl 1:S25-30.

34. Wypij JM, Fan TM, Fredrickson RL, Barger AM, de Lorimier LP, Charney SC. In vivo and in vitro efficacy of zoledronate for treating oral squamous cell carcinoma in cats. J Vet Intern Med 2008;22(1):158-63.

35. Coxon FP, Rogers MJ. The role of prenylated small GTP-binding proteins in the regulation of osteoclast function. Calcif Tissue Int 2003;72(1):80-4.

36. Tada T, Shin M, Fukushima H, et al. Oral squamous cell carcinoma cells modulate osteoclast function by RANKL-dependent and -independent mechanisms. Cancer Lett 2009;274(1):126-31.

37. Reid IR. Osteonecrosis of the jaw: Who gets it, and why? Bone 2009;44(1):4-10.

38. Edwards BJ, Gounder M, McKoy JM, et al. Pharmacovigilance and reporting oversight in US FDA fast-track process: Bisphosphonates and osteonecrosis of the jaw. Lancet Oncol 2008;9(12):1166-72.

Legends for illustrations:

Figure 1. ZOL treatment reduced SCCF2Luc xenograft growth.

A, Six representative mice from each group are shown, illustrating the bioluminescent image following 28 days of treatment. B, Mice were imaged at day 1,7,21 and 28 days of treatment. The fold change in radiance was determined for each mouse by dividing the ROI radiance values on days 7, 21 and 28 by the initial ROI values from day 1. On day 28, the fold change radiance was reduced 43% in ZOL-treated mice compared to vehicle treated mice (*P=0.004).

Figure 2. ZOL reduced SCCF2Luc xenograft area.

Histomorphometric evaluation of histologic tumor sections revealed that ZOL-treatment reduced adjusted tumor area (total area minus areas of necrosis) by 14% (*P=0.0375).

Figure 3. ZOL inhibited SCCF2Luc xenograft-induced osteolysis.

A, Faxitron radiography (post mortem, mandibles removed) of 3 representative mice from each treatment group (xenograft margins = white arrows, osteolysis = red arrows, new bone formation = blue asterisks). Zoledronic acid treatment was associated with reduced osteolysis and increased periosteal new bone formation compared to vehicle treated mice. B, Images representing 3 dimensional renderings of microcomputed tomography (μCT) data. Normal premaxillary bone (white arrow) and maxillary bone (blue arrow) are indicated on the Sham + Vehicle mouse. SCCF2Luc xenografts in vehicle treated mice were associated with marked loss of lateral pre-maxillary and maxillary bone revealing the root of the maxillary incisor (red arrows). Zoledronic acid treatment resulted in reduced osteolysis of maxillary and premaxillary bone (minimal exposure of incisor root, red circle) and increased periosteal new bone formation. C, A 2mm thick region of interest (ROI) incorporating pre-maxillary and maxillary bone was selected using μCT and image analysis software (red band), allowing bone surface area and bone volume to be

calculated and compared between treatment groups.

Figure 4. ZOL prevented loss of bone surface area and bone volume in SCCF2Luc xenograft bearing mice.

SCCF2Luc xenograft growth resulted in a significant reduction in bone surface area (13.9%, *P<0.0001) and bone volume (18.9%, *P<0.0001) compared to non-tumor bearing mice. ZOL prevented loss of bone surface area and bone volume (no statistically significant difference between ZOL-only mice and ZOL-SCCF2Luc tumor-bearing mice).

Figure 5. ZOL reduced histologic evidence of SCCF2Luc-associated osteolysis.

A, SCCF2Luc xenografts were associated with marked osteolysis of the adjacent premaxillary and maxillary bone (white asterisks) along the infiltrating front of the tumor (black arrows, bar = 500μm). B, Higher magnification from Panel A (box), illustrating islands of squamous cell carcinoma cells (arrows) infiltrating the remaining bone (white asterisk, bar = 100μm). C, Treatment with zoledronic acid resulted in reduced resorption of premaxillary and maxillary bone (black asterisks, Bar = 500μm). Despite reduced bone resorption, higher magnification (D) reveals islands of squamous cell carcinoma cells infiltrating the bone and the periodontal ligament (black arrows, bar = 100μm). Frequency of SCCF2Luc xenograft invasion into the skull was similar in both groups of mice. There was no difference in the incidence of xenograft invasion between vehicle-treated and ZOL-treated mice.

Figure 6. ZOL-mediated sparing of bone loss was characterized by reduced loss of preexisting bone balanced by increased new bone formation.

SCCF2Luc xenografts were associated with a 47.7% reduction in total bone area (preexisiting bone and new bone combined) compared to the non-tumor bearing side (*P=0.0002), whereas ZOL treatment prevented loss of total bone area. Xenograft growth was associated with a 64.1%

reduction in preexisting bone (*P=0.0003) in vehicle treated mice, however loss of preexisiting bone was reduced to 33.3% in ZOL-treated mice (*P=0.0001). ZOL treated mice retained 2-fold more preexisiting bone compared to vehicle treated mice (*P=0.005). The preservation of total bone in ZOL-treated mice is attributed to reduced loss of preexisting bone and increased new bone formation.

Figure 7. ZOL reduced the number of bone-resorbing osteoclasts at the tumor-bone interface.

Histomorphometric evaluation of TRAP-stained slides revealed no difference in the percentage of eroded bone between ZOL and vehicle treated mice, however the percentage of bone in direct contact with activated osteoclasts to total bone surface was reduced by 33.4% (*P=0.017). ZOL reduced the number of osteoclasts per millimeter by 51.8% (*P=0.0001). The average osteoclast length was increased in the ZOL-treated mice by 39.1% (*P=0.0001).

Figure 8. Osteoclasts in ZOL-treated mice were characterized by vacuolar degeneration.

Osteoclasts were multinucleated (small black arrows), and in ZOL-treated mice were characterized by vacuolar degeneration (large black arrows). Islands of FOSCC are indicated by 'T'.

Figure 9. ZOL failed to reduce plasma PTHrP in mice bearing SCCF2Luc xenografts.

Plasma PTHrP was elevated in tumor bearing mice (2.42 pM) compared to control mice (0.65pM, *P=0.037); however ZOL treatment did not significantly reduce plasma PTHrP values. Xenograft growth and ZOL-treatment had no effect on plasma calcium compared to control mice.

Illustrations:

Figure 1. ZOL treatment reduced SCCF2Luc xenograft growth.

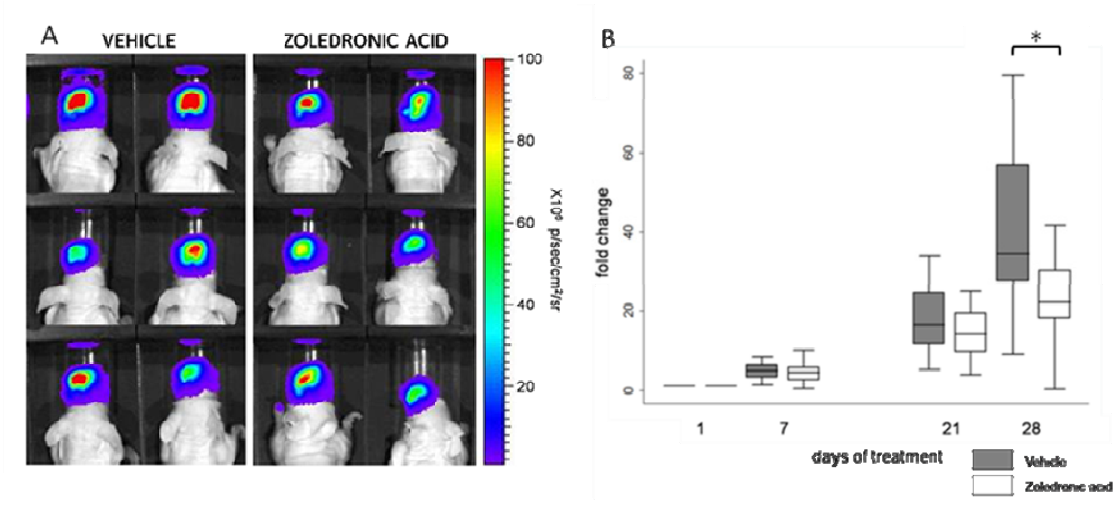

Figure 2. ZOL reduced SCCF2Luc xenograft area.

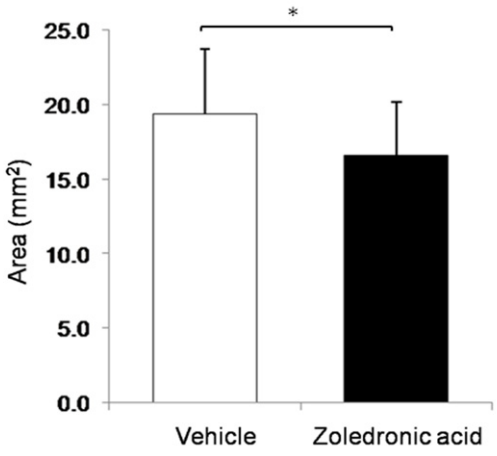

Figure 3. ZOL inhibited SCCF2Luc xenograft-induced osteolysis.

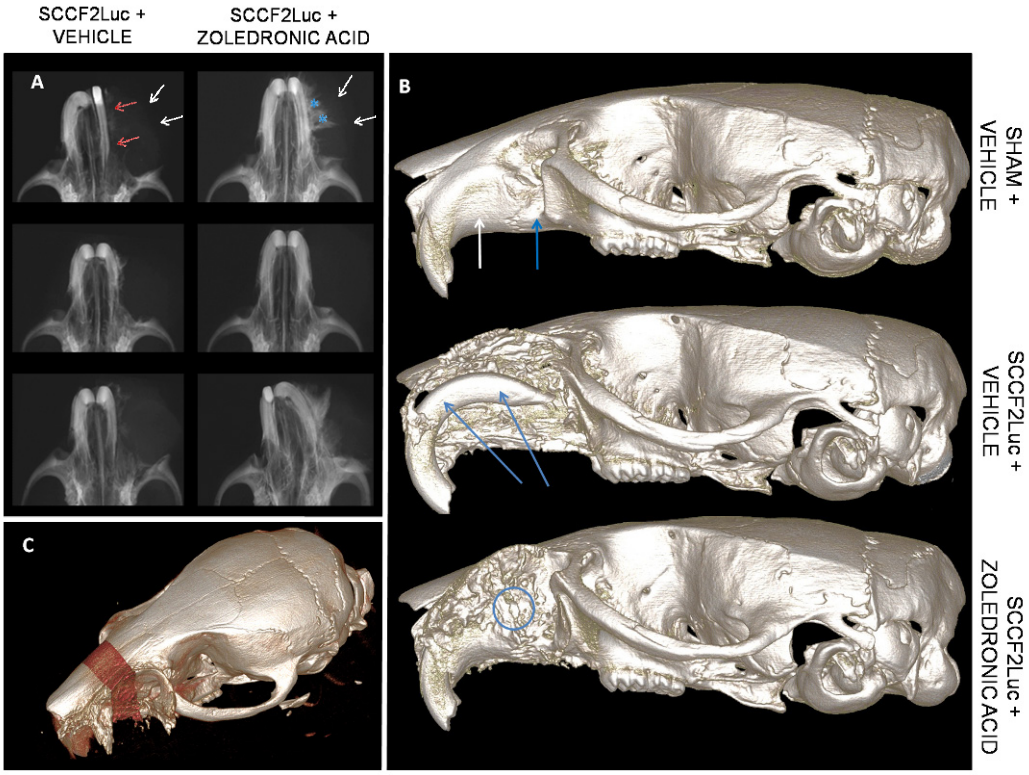

Figure 4. ZOL prevented loss of bone surface area and bone volume in SCCF2Luc xenograft bearing mice.

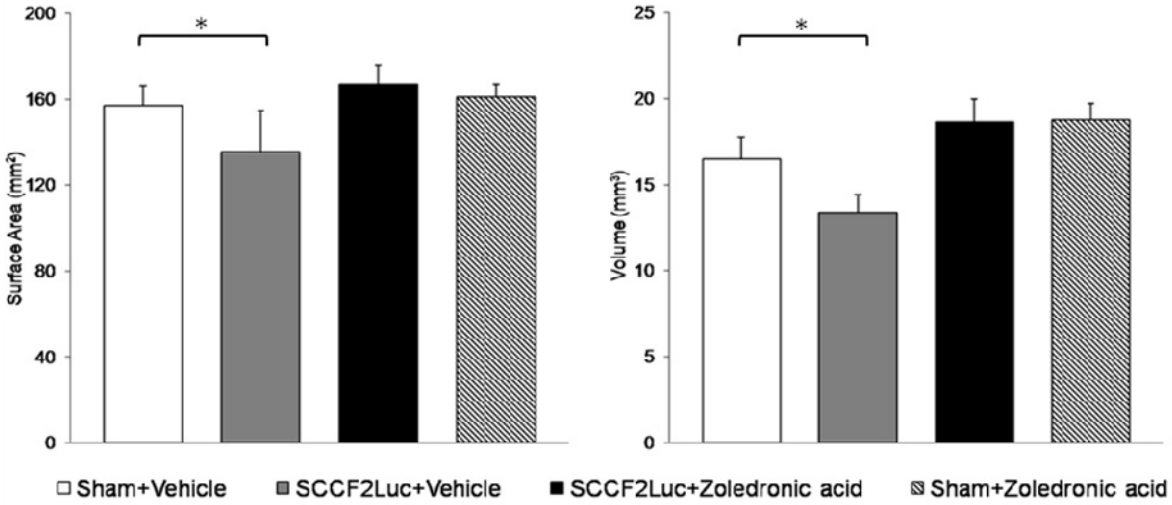

Figure 5. ZOL reduced histologic evidence of SCCF2Luc-associated osteolysis.

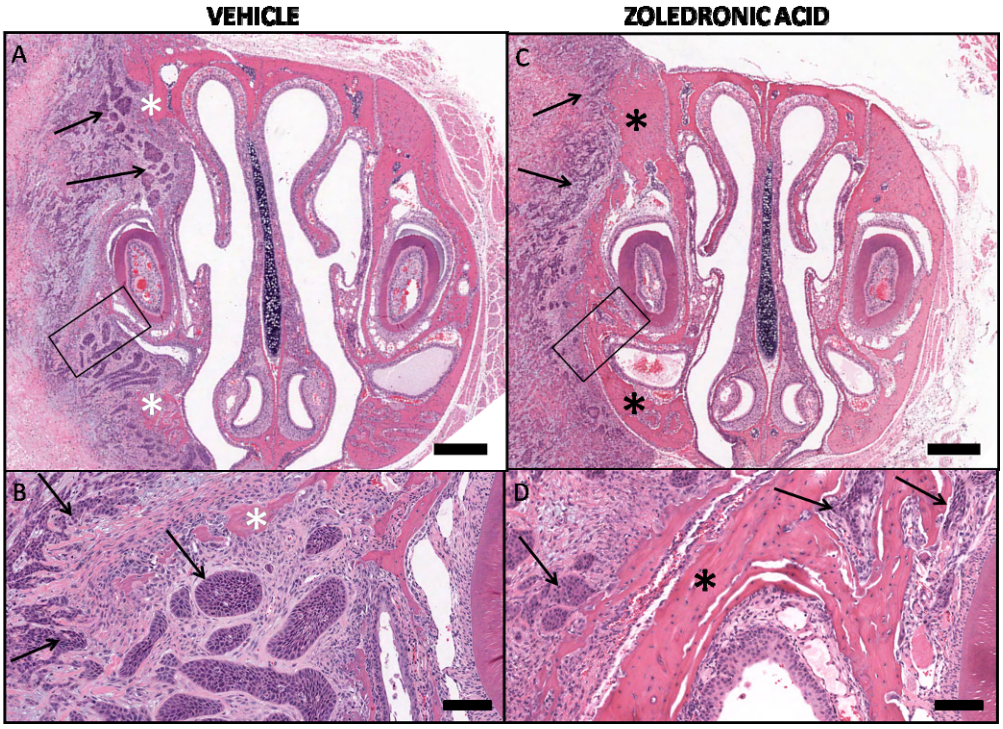

Figure 6. ZOL-mediated sparing of bone loss was characterized by reduced loss of preexisting bone balanced by increased new bone formation.

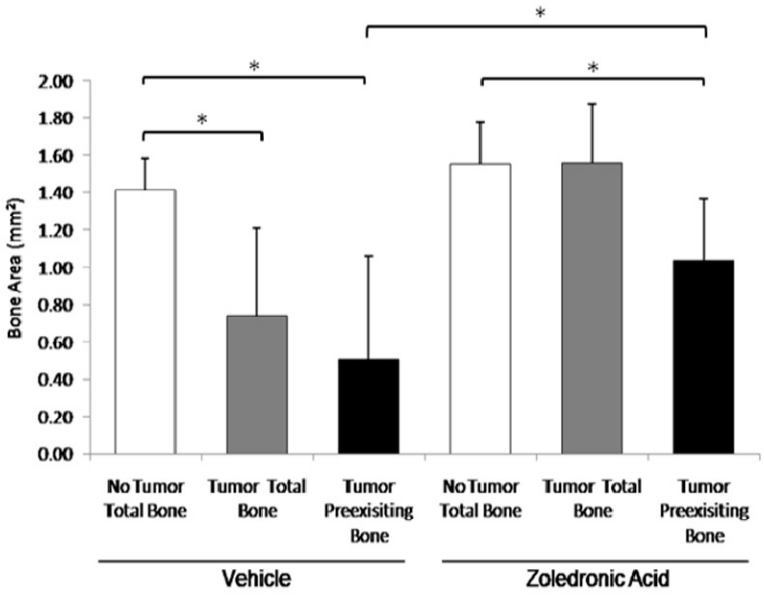

Figure 7. ZOL reduced the number of bone-resorbing osteoclasts.

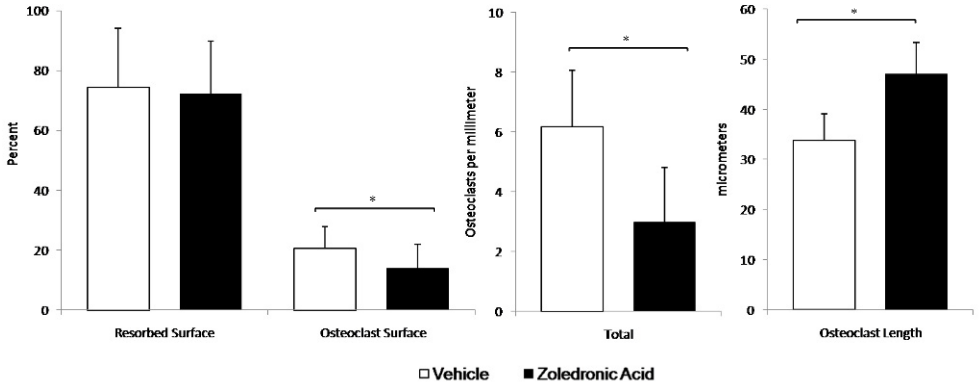

Figure 8. Osteoclasts in ZOL-treated mice were characterized by vacuolar degeneration.

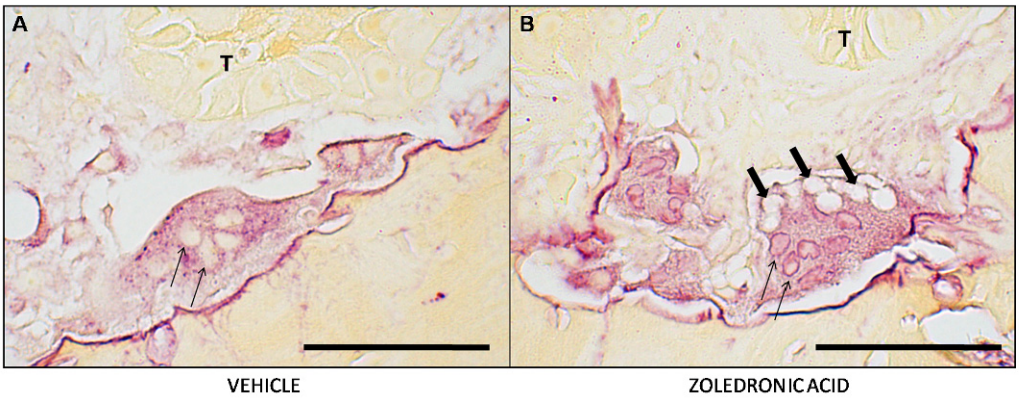

Figure 9. ZOL failed to reduce plasma PTHrP in mice bearing SCCF2Luc xenografts.